Band-structure effects on Landau-level mixing in resonant magnetotunneling

D.-Y. Lin, C.-W. Chen, and G. Y. Wu*

Department of Electrical Engineering, National Tsing-hua University, Hsin-chu, Taiwan, Republic of China

We perform a $\mathbf{k} \cdot \mathbf{p}$ calculation including both strain and band-structure anisotropy for a Si/SiGe double-barrier structure, and show in the absence of scattering that a longitudinal magnetic field can induce satellite peaks in the I-V curve. We analyze the resonant-magnetotunneling experiment of Zaslavsky *et al.*, in which two such peaks were reported, and show that the stronger peak is due to the mixing of Landau levels (with $\Delta n = 3$) caused by the coupling between heavy and light holes. On the other hand, our theory shows that the band-structure anisotropy can induce a weak peak at a low bias, which is consistent with the experiment. Our calculation demonstrates that the Landau-level mixing produced by band-structure effects can be quite large compared with that due to phonon or impurity scattering. [S0163-1829(98)07507-9]

I. INTRODUCTION

Resonant tunneling in a double-barrier resonant-tunneling structure (DBRTS) was first reported by Chang, Esaki, and Tsu, which occurs through a quasilevel in the well.[1] Later, Mendez, Esaki, and Wang observed, in the presence of a longitudinal magnetic field, resonant magnetotunneling, which occurs via Landau levels in the well.[2] Since this work, resonant magnetotunneling has become an important tool with which impurity scattering and LO-phonon-assisted resonant tunnelings have been resolved.[3,4] In particular, these experiments reported observation of satellite peaks that correspond to the Landau index-nonconserving ($\Delta n \neq 0$) tunneling through a well state with its Landau index different from that of the emitter state.[4] However, since it usually involves impurity or phonon scatterings, the $\Delta n \neq 0$ tunneling is an order-of-magnitude weaker than the $\Delta n = 0$ process, which produces the primary peaks in the current-voltage curve.

Recently, Schuberth, Abstreiter, and Gornik also reported observation of Landau levels in the derivatives of the tunneling characteristics, for a p-type strained Si/SiGe DBRTS.[5] In magnetotunneling measurements on similar Si/SiGe DBRTS, Zaslavsky *et al.* further reported two satellite peaks that are induced by the magnetic field.[6] The stronger satellite peak at the high bias increases rapidly with the magnetic field, with a strength comparable to the main peak at $B = 30$ T, while the weak satellite peak at the low bias is much smaller than the main peak even at $B = 30$ T. In view of its strength, the stronger peak is obviously not induced by impurity scattering or phonon scattering, but has to do with the complicated valence-band structure itself.[6] Moreover, voltages of both satellite peaks shift quasilinearly with the magnetic field, displaying a Landau-level structure. In this article, we carry out a $\mathbf{k} \cdot \mathbf{p}$ calculation to investigate the effect of band structures on magnetotunneling. We compare our calculation with the experiment of Zaslavsky *et al.*, and clarify the origin of the stronger peak. Our calculation also includes the band-structure anisotropy, which we show can induce a weak peak in the current-voltage curve.

II. BAND-STRUCTURE EFFECTS

We shall first argue that index-nonconserving tunneling can occur without the assistance of any scattering, when there are band structure anisotropy, or coupling between heavy holes (nh) and light holes (lh). We shall use the anisotropy as an example. Let us consider a DBRTS in a magnetic field applied in the growth (z) direction. The orbit of a state in a layer obeys, in k space, the semiclassical Bohr and Sommerfeld quantization rule

$$S(\varepsilon, k_z) = 2\pi(|e|B/\hbar)n, \quad (1)$$

on a constant energy surface of energy ε, where n is an integer, S is the area enclosed by the orbit, and B is in the z direction.[7] States in different layers have to be matched at each interface. In the case of an n-type structure, where the parabolic-band model holds, the quantized state in each layer is a circular orbit characterized by an index n. Since only layer states with the same index have orbits of the same shape to match, this leads to index-conserving tunneling. The conservation of index is broken only in the presence of some scatterings. But, if warping is present in the xy cross section of the energy surface, as is the case of a p-type structure, and if it varies from layer to layer, it is not possible to match states of the same index because their orbits are different in shape.[8] In this case, layer orbitals mixing states of different indices have to be formed and matched at the interface. This leads to index-mixing tunneling even in the absence of any scattering.

III. THEORETICAL MODEL

The envelope-function theory has been developed to treat semiconductor layered structures.[9] It has been extended to include the effect of a magnetic field.[10–16] In particular, in Ref. 15, superlattice band structures have been calculated with a multiband envelope-function theory, within the approximation of band-structure isotropy.

We now include the anisotropy in the multiband theory and calculate resonant magnetotunneling in a DBRTS. We take the magnetic field to be in the z direction, the growth direction of the DBRTS. The vector potential is chosen to be

$$\mathbf{A} = (-By, 0, 0). \quad (2)$$

<u>57</u>   4599

We shall explore the effect of anisotropy on the solution of the Hamiltonian equation for this system. We write the Hamiltonian as the sum

$$H = H_i + H_s + H_a, \tag{3}$$

where H_s is the strain interaction, H_i is the isotropic part, which, in the absence of magnetic field, results in a cylindrically symmetric band structure, and H_a is the anisotropic part. H_s has been given by Ref. 15, and, hence, is not repeated here. H_a and H_i were also given before,[15,17,18] but since they will be referred to in the discussion, we shall describe them briefly in the Kramer $|J,M\rangle$ basis, with $|U_1\rangle = \text{hh}\uparrow$, $|U_2\rangle = \text{lh}\uparrow$, $|U_3\rangle = \text{so}\uparrow$, $|U_4\rangle = \text{lh}\downarrow$, $|U_5\rangle = \text{hh}\downarrow$, and $|U_6\rangle = \text{so}\downarrow$. We write the wave function in the lth layer of the DBRTS as the linear combination

$$|k_x,l\rangle = \sum_N |N;k_x,l\rangle, \tag{4}$$

where

$$|N;k_x,l\rangle = \sum_d C_{d,N}^{(l)} e^{ik_x x} h_{n(N,d)}(y - \hbar k_x/eB)|U_d\rangle, \tag{5}$$

with $h_{n(N,d)}$ a harmonic oscillator function of index n. Specifically, we have $n(N,1)=N$, $n(N,2)=N+1$, $n(N,3)=N+1$, $n(N,4)=N+2$, $n(N,5)=N+3$, and $n(N,6)=N+2$, with N an integer ≥ -3. Notice that H_i is N-diagonal, i.e., $\langle N;k_x,l|H_i|N',k_x,l\rangle \sim \delta_{NN'}$,[15,17,18] but couples different hole states, and, within the $J=3/2$ subspace containing only hh and lh states, the upper triangular part of H_i is[19]

$h_N|\text{hh}\uparrow\rangle$	$h_{N+1}|\text{lh}\uparrow\rangle$	$h_{N+2}|\text{lh}\downarrow\rangle$	$h_{N+3}|\text{hh}\downarrow\rangle$
$P_1N + G_1$	$iQ\sqrt{N+1}$	$S\sqrt{(N+1)(N+2)}$	0
	$P_2(N+1) + G_2$	0	$S\sqrt{(N+2)(N+3)}$
		$P_2(N+2) + G_3$	$-iQ\sqrt{N+3}$
			$P_1(N+3) + G_4.$

$$\tag{6}$$

P_i's, G_i's, Q, and S are just functions of B and $-i\partial/\partial z$.[20] For the anisotropic part, we have

$$H_a = \begin{bmatrix} 0_{3\times3} & \Pi_a \\ \Pi_a^+ & 0_{3\times3} \end{bmatrix}, \tag{7}$$

where

$$\Pi_a = -\frac{\sqrt{3}}{2}\frac{\hbar eB}{m}(\gamma_2 - \gamma_3)a^{+2} \begin{bmatrix} 1 & 0 & -i\sqrt{2} \\ 0 & 1 & 0 \\ 0 & -i\sqrt{2} & 0 \end{bmatrix}, \tag{8}$$

with

$$a^+ = \sqrt{1/2eB\hbar}(\hat{p}_x - eBy + i\hat{p}_y). \tag{9}$$

The presence of H_a couples the state $|N;k_x,l\rangle$ with $|N\pm4;k_x,l\rangle$, $|N\pm4;k_x,l\rangle$ with $|N\pm8;k_x,l\rangle$, and so on, which follows from the forms of H_a and $|N;k_x,l\rangle$. In the numerical calculation, we shall make the lowest-order approximation to the anisotropy by retaining only the direct coupling between $|N;k_x,l\rangle$ and $|N\pm4;k_x,l\rangle$. There is only indirect coupling between $|N;k_x,l\rangle$ and $|N\pm8;k_x,l\rangle$, for example, which is induced by their direct coupling to $|N\pm4;k_x,l\rangle$. Since this is a higher-order effect, we neglect it in the calculation.

The coefficients $C_{d,N}^l$ in Eq. (5) for each layer are determined by the interface boundary condition that the wave function and its derivative are continuous at each interface. This results in a transfer-matrix equation. We then solve for $C_{d,N}^l$ and calculate transmission coefficients for electrons incident with various energies. Summing all transmissions of the Fermi sea gives tunneling currents. The same transfer matrix formulation can be used to obtain bound states of a quantum well. Details of the formulation for the calculation of tunneling and bound states in a multiband model can be found in Ref. 20.

From the Hamiltonian given in Eqs. (6)–(8), it is obvious that index-mixing tunneling can occur in various ways, because there are several nonvanishing matrix elements between states of different harmonic-oscillator indices. However, for the tunneling to be observable, it must be strong enough. Since the emitter particles in the case concerning us are primarily heavy holes (see Sec. IV below), it will be most favorable for the hh to mix in the lh. There are two ways for it to happen. One is via the hh-lh coupling contained in H_i of Eq. (6), which we shall term as the H_i-induced hh-lh coupling, and the other is via a similar coupling caused by $(\Pi_a)_{22}$ contained in H_a, which shall be called the H_a-induced hh-lh coupling. With the decay of a lh wave function in the barrier being slower than that of a hh, it is easier to observe the index-mixing tunneling of an emitter hh through barriers via the lh channel than via the hh channel.

IV. RESULTS AND CONCLUSION

We carry out the calculation for a symmetric Si/Si$_{0.75}$Ge$_{0.25}$ DBRTS system, with the barrier width 50 Å, and well width 35 Å. Si layers are barriers, and Si$_{0.75}$Ge$_{0.25}$ layers form the emitter, quantum well, and collector. The Fermi energy is 6.1 meV at $B = 30$ T, and varies with the magnetic field. The in-plane lattice constant is taken to be that of Si, which imposes a biaxial strain in the Si$_{0.75}$Ge$_{0.25}$ layers. These structural parameters are chosen so that the system resembles one of the structures probed in Ref. 6.
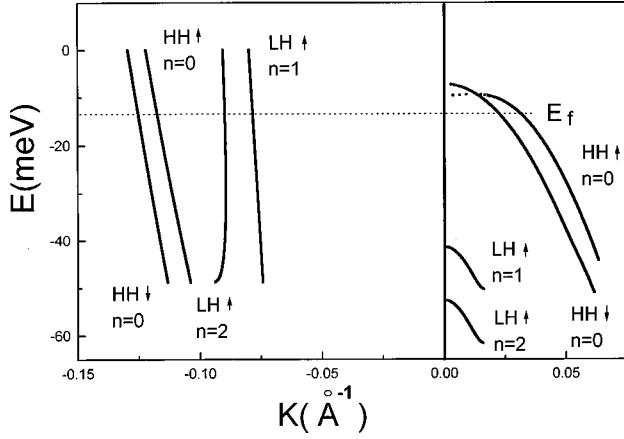
FIG. 1. On the right is energy vs the real part of wave vector, for $Si_{0.75}Ge_{0.25}$. On the left is energy vs the imaginary part of wave vector, for Si. The magnetic field is 30 T. The two band structures are aligned according to the band offset.

FIG. 2. Current-voltage curves. Filled squares are the calculated data. The curves for $B=25$ T and $B=30$ T have been shifted vertically.

However, ours does not include spacer layers as the experimental structure does. For the Luttinger parameters of Si, we take $\gamma_1 = 4.22$, $\gamma_2 = 0.39$, $\gamma_3 = 1.44$, and $\kappa = -0.26$, and, for Ge, we take $\gamma_1 = 13.35$, $\gamma_2 = 4.25$, $\gamma_3 = 5.69$, and $\kappa = 3.41$.[21] For band offset, elastic constants, and deformation potentials, we also use that of Ref. 21. Some adjustment of the parameters, however, has been made.[22]

In Fig. 1, we present the bulk complex band structures for the constituent materials Si and $Si_{0.75}Ge_{0.25}$. We show only the bands involved in the calculation. In the range 20 T$<B$ $<$30 T, only the lowest $n=0$ hh Landau levels are occupied in the emitter, and, hence, they are the states whose tunneling behavior we shall focus on. We note that the $n=0$ hh↑ band couples with both the $n=1$ lh↑ and $n=2$ lh↓ bands, a consequence of the H_i-induced coupling, and that the $n=0$ hh↓ band couples with the $n=2$ lh↑ band, a consequence of the H_a-induced coupling. We also see that, in the barrier, the lh wave vectors are smaller in magnitude than the hh ones, indicating a slower decay of the lh wave. To compare the magnitude of mixing induced by H_i with that by H_a, we list here some major $|C_{d,n}|$'s of the emitter states at the Fermi level, with $B=30$ T. For the $n=0$ hh↑ state, we have

$$|C_{hh\uparrow n=0}| = 0.9387, \quad |C_{lh\uparrow n=1}| = 0.2874,$$

$$|C_{lh\downarrow n=2}| = 0.046.$$

For the $n=0$ hh↓, we have

$$|C_{hh\uparrow n=0}| = 0.9988, \quad |C_{lh\uparrow n=2}| = 0.0339.$$

From above, we see that the H_a-induced mixing is much weaker than the H_i-induced mixing. Correspondingly, it implies that the H_a-induced index-nonconserving tunneling is much weaker than the H_i-induced one. The explanation for this is the following. The hh-lh coupling in H_i increases with the magnetic field, and, at $B=30$ T, the coupling is so large that hh and lh strongly mix. On the other hand, the hh-lh

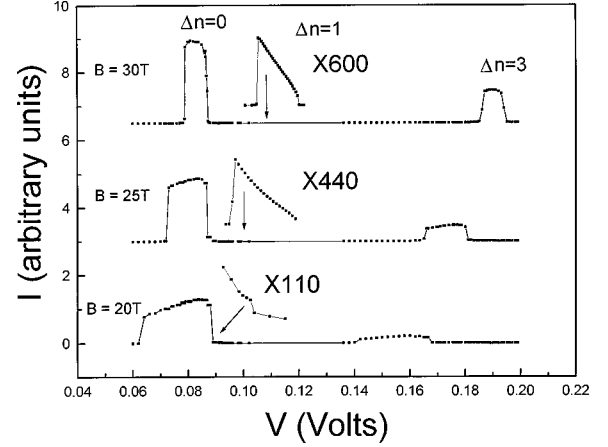coupling in H_a is relatively insensitive to the variation of magnetic field, and is mainly determined by the anisotropy at $B=0$, which is small.

In Fig. 2, we present the current-voltage curve. Notice the appearance of two index-nonconserving tunneling peaks, denoted as $\Delta n=1$ and $\Delta n=3$, respectively, in addition to the primary peak denoted as $\Delta n=0$. The $\Delta n=3$ peak grows rapidly with magnetic field, and, at $B=30$ T, it is of the same order of magnitude as the $\Delta n=0$ peak. The primary peak is due to the resonant tunneling of the emitter $n=0$ hh↑($\downarrow$) state through the $n=0$ hh↑($\downarrow$) state in the well. We have also determined the well states that the two index-nonconserving tunnelings utilize. We list below their energies together with the major $|C_{d,n}|$'s of their wave functions, with $B=30$ T. One state has

$$E = -61 \text{ meV}, \quad |C_{hh\uparrow n=1}| = 0.9296, \quad |C_{lh\uparrow n=2}| = 0.2458,$$

which is primarily an $n=1$ hh↑ state coupled with an $n=2$ lh↑ state. The other state has

$$E = -95.5 \text{ meV}, \quad |C_{hh\downarrow n=3}| = 0.8012, \quad |C_{lh\uparrow n=1}| = 0.4499,$$

which is primarily an $n=3$ hh↓ state coupled with an $n=1$ lh↑ state. In the above, the zero energy is taken to be at the heavy-hole band edge. Combining the foregoing analyses of emitter and well wave functions, we conclude that the $\Delta n=1$ tunneling occurs with the following sequence of steps

emitter	coupled via	barrier	coupled via	well
$n=0$ hh↓	H_a	$n=2$ lh↑	H_i	$n=1$ hh↑.

Since the difference between the Landau indices of the emitter and well states is 1, we identify the index change as $\Delta n=1$. On the other hand, the $\Delta n=3$ tunneling occurs with the following sequence of steps

emitter	coupled via	barrier	coupled via	well
$n=0$ hh↑	H_i	$n=1$ lh↑	H_i	$n=3$ hh↓.

Since the difference between the Landau indices of the emitter and well states is 3, we identify the index change as $\Delta n = 3$. With the $\Delta n = 1$ tunneling induced by H_a and the $\Delta n = 3$ tunneling induced by H_i, the $\Delta n = 1$ peak is much weaker than the $\Delta n = 3$ peak.

Comparing this figure with the I-V curve of Zaslavsky *et al.*, we identify the $\Delta n = 3$ peak with the stronger satellite peak that they observed. On the other hand, the $\Delta n = 1$ peak, although appearing in our curve, is too weak when compared with their weaker satellite peak. We therefore do not exclude the possibility that the experimental peak could be due to scattering-assisted tunneling, or other mechanisms. However, the weakness of the theoretical $\Delta n = 1$ peak is at least consistent with the experimental result.

In Fig. 3, we present the shift of voltages at current peaks with magnetic field.[23] As we can see, it goes almost linearly with the magnetic field. Moreover, the slope, $\Delta V / \Delta B$, for the $\Delta n = 3$ peak, is about 3 times of that for the $\Delta n = 1$ peak, after subtracting the slope for the main peak (with $\Delta n = 0$) from them.[24]

In conclusion, we have performed a $\mathbf{k} \cdot \mathbf{p}$ calculation that includes both strain and band-structure anisotropy, for a Si/SiGe double-barrier structure, and show, in the absence of scattering, that a longitudinal magnetic field can induce satellite peaks in the I-V curve. We have compared the calculation with the resonant-magnetotunneling experiment of Zaslavsky *et al.*, and shown that the stronger peak is due to the mixing of Landau levels (with $\Delta n = 3$) caused by the
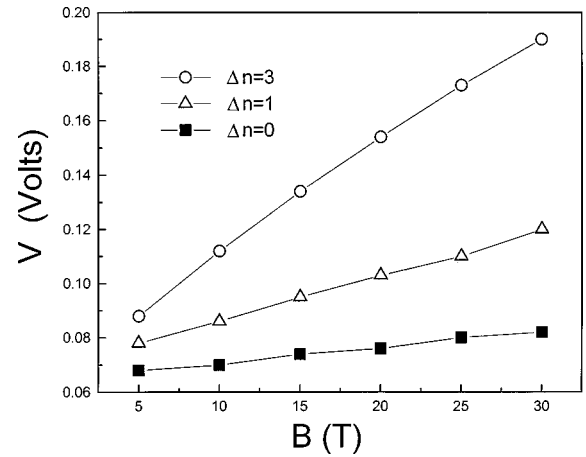

FIG. 3. Center positions of current peaks vs magnetic field.

H_i-induced coupling between heavy and light holes. Our theory has also shown that the band structure anisotropy can induce a weak peak at low bias, which is consistent with the experiment. Our calculation has demonstrated that the Landau-level mixing produced by band-structure effects can be quite large compared with that due to phonon or impurity scattering.

*Author to whom correspondence should be addressed. Also at Department of Physics, National Tsing-Hua University, Hsin-Chu, Taiwan.

[1] L. L. Chang, L. Esaki, and R. Tsu, Appl. Phys. Lett. **24**, 593 (1974).

[2] E. E. Mendez, L. Esaki, and W. I. Wang, Phys. Rev. B **33**, 2893 (1986).

[3] V. J. Goldman, D. C. Tsui, and J. E. Cunningham, Phys. Rev. B **36**, 7635 (1987).

[4] M. L. Leadbeater, E. S. Alves, L. Eaves, M. Henini, O. H. Hughes, A. Celeste, J. C. Porter, G. Hill, and A. Pate, Phys. Rev. B **39**, 3438 (1989).

[5] G. Schuberth, G. Abstreiter, and E. Gornik, Phys. Rev. B **43**, 2280 (1991).

[6] A. Zaslavsky, D. A. Grutzmacher, S. Y. Lin, T. P. Smith III, R. A. Kiehl, and T. O. Sedgwick, Phys. Rev. B **47**, 16 036 (1993).

[7] See, for example, L. D. Landau and E. M. Liftshitz, *Course of Theoretical Physics* (Maxwell, M. C., 1977), Vol. 9, p. 241.

[8] Warping normally depends on energy. For example, in the limit of large spin-orbit splitting, heavy- and light-hole bands are approximately $\varepsilon(\vec{K}) = Ak^2 \pm [B^2k^4 + C^2(k_x^2 k_y^2 + k_y^2 k_z^2 + k_z^2 k_x^2)]^{1/2}$. See, for example, C. Kittel, *Quantum Theory of Solids* (John Wiley and Sons, Inc., New York, 1963), p. 273. Since ϵ varies as we go through a layered structure, the degree of warping changes from layer to layer.

[9] See, for example, D. L. Smith and C. Mailhiot, Phys. Rev. B **33**, 8345 (1986), and references therein.

[10] A. Fasolino and M. Altarelli, Surf. Sci. **142**, 322 (1984).

[11] G. Bastard and J. A. Brum, IEEE J. Quantum Electron. **22**, 1625 (1986).

[12] S. Lamari and L. J. Sham, Surf. Sci. **196**, 551 (1988).

[13] J. C. Maan, Surf. Sci. **196**, 518 (1988).

[14] J. A. Brum, P. Voisin, M. Voos, L. L. Chang, and L. Esaki, Surf. Sci. **196**, 545 (1988).

[15] G. Y. Wu, T. C. McGill, C. Mailhiot, and D. L. Smith, Phys. Rev. B **39**, 6060 (1989).

[16] T.-J. Chow, G. Y. Wu, K.-M. Hung, and C.-W. Chen, Phys. Rev. B **55**, 1329 (1997).

[17] C. R. Pidgeon and R. N. Brown, Phys. Rev. **146**, 575 (1966).

[18] W. Leung and L. Liu, Phys. Rev. **146**, 575 (1966).

[19] This is only what we need for discussion. However, in the numerical calculation, we use the full H_i as given in Refs. 15, 17, and 18, which is a 6×6 matrix.

[20] G. Y. Wu, K.-M. Hung, and C.-J. Chen, Phys. Rev. B **46**, 1521 (1992).

[21] Y. Fu, S. C. Jain, M. Willander, and J. J. Loferski, J. Appl. Phys. **74**, 402 (1993), and references therein.

[22] The Luttinger parameters we take are off by within 20% from that obtained by a linear interpolation between those of Si and Ge, and so are the deformation-potential parameters. For the strained Si/Si$_x$Ge$_{1-x}$ system, a straight linear interpolation of the parameters does not work well. See Ref. 6 and also J.-P. Cheng, V. P. Kesan, D. A. Grutzmacher, and T. O. Sedgwick, Appl. Phys. Lett. **62**, 1522 (1993). Another reason for our adjustment of parameters is that we have neglected spacer layers and Coulomb interaction between the carriers.

[23] The peak's center is actually determined approximately by a calculation of the transmission-bias curve, $T(V)$, where the incident state is set at $\frac{1}{2} E_f$, whose tunneling behavior is typical of that of an emitter carrier. Since $I(V)$ differs from $T(V)$ roughly

by only a factor of the emitter's density of states, which is a smooth function, the two functions resemble each other. We therefore take the transmission peak position to be the center of the corresponding current peak. This saves a lot of CPU time because the calculation of $T(V)$ is much faster.

[24] Although Zaslavsky *et al.* identified their stronger peak as $\Delta n = 2$, its slope, $\Delta V/\Delta B$ at low B, according to their data, is more than 2.5 times that for the $\Delta n = 1$ peak.